Ore Geology Reviews 101 (2018) 675–687

Contents lists available at ScienceDirect

Ore Geology Reviews

journal homepage: www.elsevier.com/locate/oregeorev

Monitoring surface mining belts using multiple remote sensing datasets: A global perspective

Le Yu[a,b,*], Yidi Xu[a], Yueming Xue[c], Xuecao Li[d], Yuqi Cheng[a], Xiaoxuan Liu[a], Alok Porwal[e,f], Eun-Jung Holden[f], Jian Yang[g], Peng Gong[a,b]

[a] Ministry of Education Key Laboratory for Earth System Modeling, Center for Earth System Science, Tsinghua University, Beijing 100084, China
[b] Joint Center for Global Change Studies, Beijing 100875, China
[c] China Institute of Geo-Environmental Monitoring, Beijing 100081, China
[d] Department of Geological and Atmospheric Sciences, Iowa State University, Ames, IA, USA
[e] Centre of Studies in Resources Engineering, Indian Institute of Technology Bombay, Powai, 400076 Mumbai, India
[f] Centre for Exploration Targeting, School of Earth Sciences, The University of Western Australia, Crawley 6009, WA, Australia
[g] Department of Forestry, University of Kentucky, Lexington, KY 40546, USA

ARTICLE INFO

Keywords:
Change detection
Surface mining
Time series
Global

ABSTRACT

Quantifying the spatiotemporal change of land cover and understanding their ecological, environmental, and socioeconomic impacts are important for sustainable development. Surface mining by the minerals industry is one driver of the changes in land cover, leading to loss of natural vegetation and top soils, and interruption of ecosystem service flows. This study investigates the effectiveness of remote sensing datasets to identify and map land cover changes, with the specific goal of understanding the impact of surface mining activities on land cover globally from 1980s to 2013. Diverse remote sensing datasets with long term observations are analyzed, including high-resolution images in Google Earth, Landsat Thematic Mapper (TM)/Enhanced Thematic Mapper Plus (ETM+)/Operational Land Imager (OLI), the Moderate Resolution Imaging Spectroradiometer (MODIS) Vegetation Index (VI) product and Defense Meteorological Satellites Program (DMSP)/Operational Linescan System (OLS) stable night-time light. The results indicated that after entering 21st century, North America (e.g., the United States and Canada) was the only continent to have more surface mining spots categorized as Shrink type (rehabilitated) rather than Expand type. South America (e.g., Chile and Brazil) and Asia (e.g., India and China) had the highest proportions of Expand Type of surface mining spots. Detailed demonstrations on how those remote sensing datasets could help in mining spot monitoring are presented.

1. Introduction

Rapid economic and social development drives growing demands for mineral resources. However, mining of these resources has a significant impact on ecological environment as mining activities take up land resources, leading to the destruction of arable land and vegetation (Schueler et al., 2011; Townsend et al., 2009); destroying the natural landscape and affecting the integrity of the ecosystem and local biodiversity (Antwi et al., 2008); producing emissions from mining which cause atmosphere/water/soil pollution; and inducing a variety of geological disasters, such as debris flow and landslides (Latifovic et al., 2005). In particular, monitoring of land use/cover changes and its consequences for ecological, environmental, and socioeconomic impact on Earth is critical for sustainable development.

A conventional approach to environmental monitoring for mining is based on field inspection which is slow and expensive. However, with the advances in satellite-to-ground observation technology, remote sensing technology has become an effective method (Latifovic et al., 2005; Townsend et al., 2009). Surface mining removes vegetation and soils, resulting in land cover changes. In the field of satellite remote sensing, land-cover mapping has become one of the most active areas of research (Yu et al., 2014a). Hundreds of satellites have been launched to observe land dynamics. Since the early days of satellite remote sensing, the spatial resolution of sensors on board these satellites has increased to sub-meter. The spectral sampling frequency has increased nearly a hundredfold from a few spectral bands to a few hundred bands. Rapid advancements in hardware and computing techniques made land cover monitoring at the global scale possible (e.g., Gong et al., 2013; Yu

* Corresponding author at: Ministry of Education Key Laboratory for Earth System Modeling, Center for Earth System Science, Tsinghua University, Beijing 100084, China.
E-mail address: leyu@tsinghua.edu.cn (L. Yu).

https://doi.org/10.1016/j.oregeorev.2018.08.019
Received 29 September 2017; Received in revised form 3 August 2018; Accepted 14 August 2018
Available online 16 August 2018
0169-1368/

Table 1
Datasets used in this study.

Dataset	Spatial resolution	Time period	Revisit interval	Data processing
High resolution images	< 1 m	1960s–2017	Irregular	–
Landsat	30 m	1970s–2016	16 days	Atmospheric and terrain corrected
MODIS VI	250 m	2000–2016	16 days	Poor-quality/cloud pixel were excluded
NTL	1 km	1992–2013	1 year	Inter-calibration among each year

et al., 2013, 2014b) as well as diverse applications in natural sciences, including climate and hydrological modelling, biogeochemical cycling, environmental protection, biodiversity conservation, and resource management.

For the monitoring of land cover changes with a specific focus on surface mining activity monitoring, a remote sensing based approach has many advantages over the traditional field based land cover monitoring method including the following:

- Data collection efficiency: Remote sensing technology collects surface information over a large spatial extent efficiently, while a conventional method relies on point source information where data collection is limited by access to the mine sites.
- Minimising subjectivity: Quantitative measurements from remote sensing technology are objective and repeatable unlike field work based data collection.
- Monitoring land cover dynamics: Cyclic observations by satellite remote sensing technology allow periodic updates of data from the surface mining and its surrounding areas. This allows monitoring of changes in land cover over time, i.e. land cover dynamics, which may help the understanding of land clearing and rehabilitation for the mine sites. (for mining disturbance detection and environmental impact assessment).

In the last decade, a wide range of studies have been carried out to monitor environmental impacts of mining activities (e.g. Townsend et al., 2009; Malaviya et al., 2010; Erener 2011; Schmid et al., 2013; Raval and Shamsoddini, 2014; LaJeunesse Connette et al., 2016; Redondo-Vega et al., 2017). Monitoring techniques may be based on visual interpretation or computer assisted interpretation using automated pattern recognition techniques (Latifovic et al., 2005; Petropoulos et al., 2013). The automated analysis techniques may vary, including pixel-based to object-based analysis (Bao et al., 2014; Lechner et al., 2016; Pei et al., 2017); bi-/multi-temporal image comparison; continuous time-series monitoring (Li et al., 2015; Yang et al., 2018). The monitoring may also vary depending on the details being sought within the data, from low-resolution macro-monitoring to high-resolution monitoring (Demirel et al., 2011). In recent years, Pei et al. (2017) used object-based image analysis to monitor the land cover change in a coal mining area. Yang et al. (2018) applied LandTrendr, a temporal segmentation algorithm, to dynamic monitoring of land disturbance and recovery in mine sites. Previously, many studies focused on observing detailed land cover analysis of mining area and improving the accuracy (e.g., Chen et al., 2018). However, to the best of our knowledge, no study on the long-term change of land use at the continental or global scale around the open-pit mining areas has been reported. Existing databases record the geographic coordinates, characteristics and attributes of mines at a specific time without considering the continually phasing in and out of mines (Soulard et al., 2016), therefore, keeping track of the mining-related disturbance (i.e., expansion, reclamation, or both) and updating the global database is important for environmental management and monitoring.

In this study, we applied multi-source (multi-temporal and multi-resolution) datasets, including NTL, MODIS, Landsat and high-resolution images from Google Earth, in order to globally track the spatial/temporal mining and recovery process in respect of open-pit mining of nonfuel mineral (except coal mining) resources over the past decades (1980s-2013). The specific aims of this study were: (1) to present a global surface mining dataset with accurate spatial location and changes in mining footprint, (2) to investigate the global patterns of land change in significant surface mining belts, and (3) to demonstrate the effectiveness of different remote sensing datasets in surface mining activity monitoring.

2. Datasets

This study uses long term observations of multi-source (with different spatial resolutions and revisited intervals) remote sensing images including high-resolution images in Google Earth, Landsat Thematic Mapper (TM)/ Enhanced Thematic Mapper Plus (ETM+)/Operational Land Imager (OLI), the Moderate Resolution Imaging Spectroradiometer (MODIS) Vegetation Index (VI) and Defense Meteorological Satellites Program (DMSP)/Operational Linescan System (OLS) stable nighttime light (NTL) for surface mining regions in recent decades. A summary of those datasets is shown in Table 1, and details will be elaborated in the following sections (Sections 2.2–2.5). We also used the United States Geological Survey (USGS) Major Mineral Deposits of the World (MMDW) database (https://mrdata.usgs.gov/major-deposits/) to identify the locations of surface mining areas around the world which can be used to analyse those areas' land cover changes. Images with different resolutions were given to interpreter and the change trends between vegetation and bare land for each of the identified mining spots were determined.

2.1. Deposit location data

The USGS MMDW database holds geographical locations and general geologic setting of known deposits of major nonfuel mineral commodities (Schulz and Briskey, 2005). It is compiled from five regional databases (i.e. Zientek and Orris, 2005; Cunningham et al., 2005; Peters et al., 2005; Nokleberg et al., 2005; Taylor et al., 2009) and includes information such as record ID (gid), deposit name (dep_name), country, latitude, longitude, commodity, deposit type (dep_type) and others. However, it should be noted of a level of uncertainty in this database. There are multiple authors (USGS geoscientists) for this database, there may be variations in the criteria by which deposits were chosen for inclusion. In addition, it seems mineral deposits in the United States were documented more comprehensively than in other regions, owing to better access to source materials. In addition, geographic location, the geometry and spatial extent of deposits in this database are not precise. While this study doesn't address the uncertainty in deposit selection criteria by individual authors and lack of consistency across different parts of the world in the collection of deposit data, a significant effort has been made to ensure the locations and geometry of the listed deposits and their geographic locations are validated and modified if necessary according to high-resolution images in Google Earth. Three quarters of the total sites in MMDW dataset (3161 in total) were excluded as there was no none-vegetated region (pit, overburden dumps, construction etc.) nearby based on our inspection of high resolution images. Possible reasons are (1) deposits are not necessary to be active mining sites, some may have never been mined, (2) some may have mined before but have been successfully

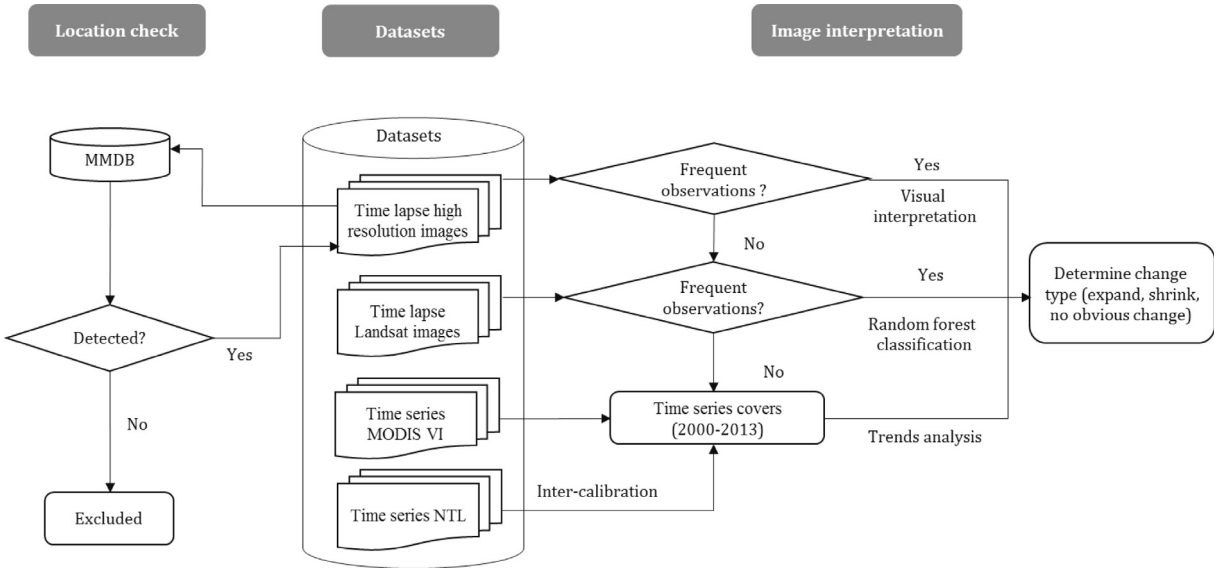

Fig. 1. Flowchart of the mining spot interpretation using multiple datasets.

reclaimed prior to the acquisition of high resolution images in Google Earth. Thus, the remaining 780 mining locations were used in our study.

2.2. High-resolution images in Google Earth

Many high-resolution images (i.e., better than 1-m resolution) have been captured and made available to trace detailed changes in land cover (Yu and Gong, 2012). The spatial coverage of high-resolution imagery in Google Earth (https://www.google.com/earth/) has been expanded rapidly in recent years. In this paper we used high-resolution images from Google Earth (mostly are SPOT 5, GEOEYE-1, IKONOS, QuickBird, Worldview-I/II and Aerial photographs) over multiple dates (from 2000 to 2016) to check for changes at specific sites according to the USGS MMDW database.

2.3. Landsat TM/ETM+/OLI

Landsat datasets (http://landsat.usgs.gov/) are one of the most widely used datasets for diverse applications, including disaster monitoring, land cover/use mapping, urban expansion, and biodiversity. The Landsat series, including TM, ETM+ and OLI, share relatively consistent reflectance bands, which helps with tracking long-term change back to the 1970s. Since the Landsat archive was made freely available to the public, Landsat images have been used for large-scale land cover mapping with a relatively fine spatial resolution (e.g., Gong et al., 2013) or subtle change detection (Xu et al., 2017). In this study, we selected the areas covering the mineral deposits from all available Landsat imagery (processing level: L1T, and atmospheric correction was done by USGS) from 1984 to 2016.

2.4. MODIS vegetation index

The MODIS dataset has coarser spatial resolution than Landsat but with more densely distributed spectral bands and a higher temporal resolution (revisiting frequency). Our study used the MODIS vegetation index (VI) data (MOD13Q1) (2001–2016) with the spatial resolution of 250 m composited every 16 days. Poor-quality pixels due to cloud cover were identified and excluded in the analysis. Analyzing a relatively long temporal span of MODIS covering the period from 2000 to 2016 every 16 days is helpful for detecting ground disturbances and understanding the change trends over time.

2.5. Night-time light (NTL)

The DMSP/OLS NTL data provides a continuous observation of nighttime luminance change caused by human-activity related events (such as socioeconomic activities or surface mining) from 1992 to 2013 (Elvidge et al., 2009). This data have a near global coverage (spanning from -180° to 180° in longitude and -65° to 65° in latitude), with a spatial resolution of 30 arc seconds (equal to 1 km at the equator). The long-term and global coverage advances the NTL dataset for detecting surface anthropogenic activities through tracking the NTL change. For this study, the NTL dataset was downloaded from the National Oceanic and Atmospheric Administration (NOAA) with the stable product (version 4) (https://ngdc.noaa.gov/eog/dmsp/downloadV4composites.html), from which ephemeral events such as fires and other background noises have been eliminated.

3. Methods

Based on the spatial and spectral attributes of the satellite datasets, various image processing and interpretation techniques were applied to track the mining disturbance through the entire time series. In the following sections, we summarize the techniques used in this study.

Three categories of changes in land-use were identified, namely, (1) expand type – changes of vegetation/bare land cover to mine site; (2) shrink type – from bare land to vegetation (rehabilitation); and (3) no obvious trend – without consistent change pattern (expand or shrink) or changes are not clearly detected. In the interpretation of the change-categories, the use of different datasets were prioritized on the basis of the spatial resolutions of the time-series images. Fig. 1 shows how the datasets at three different levels of resolution are interpreted and integrated. The priority was given first to the use of high resolution images for interpretation, and if not available, to moderate-resolution images (that is, Landsat images comprising 47.3% of the total data used in this study) and then to low resolution images (that is, VI/NTL comprising 36.8% of the data.

3.1. Visual interpretation

High resolution images from Google Earth comprising 16.9% of the data were visually interpreted for detecting the land-use change type. We checked all the high resolution time lapse images from Google Earth since 2000. This study analysed the locations of 790 mines globally and temporally dense Google Earth images were available for 128 mine

sites. The rest of the mine sites were analysed with the aid of other satellite data sources as previously shown in Fig. 1. With the aid of visual and other auxiliary information (including tone, texture, shapes etc.) using high spatial resolution and/or high temporal resolution (revisited frequency) images, we were able to identify the change type of each surface mining area. Meanwhile, since images were acquired at different time and time interval for each mining area, other satellite datasets were also used to support the discrimination of change types when temporally sparse observations (time intervals > 3 years) were available (See Sections 3.2 and 3.3). Here we supposed that mining activity is a continuous one-way activity in a short term without multi-directional change (i.e., the 1st year in shrinkage, the 2st year in expansion and 3rd year in shrinkage).

3.2. Landsat based change detection

The Landsat based mining change detection includes three main steps: pre-processing the Landsat time series, Landsat image classification and change detection based on the annual mapping results. Firstly, surface Reflectance Landsat data from 1984 to 2016 covering 47.3% mining sites was applied with atmospheric and geometric distortions correction (downloaded from United States Geology Survey, http://glovis.usgs.gov/next/) (Masek et al., 2006). Although geometrically referenced products are available from USGS, there is still offsets in a few of the Landsat images. Thus in this study, the registration accuracies of multi-temporal Landsat images were geometrically verified image-by-image using Google Earth images based on reference points such as well-defined turning points of rivers and roads. The Landsat images that were found misregistered were rejected and only geometrically consistent Landsat images were used in the next step. We used all images from Landsat TM/ETM+/OLI except for the Landsat ETM+ images that had blank scan lines. Gap-filled methods were not applied to these Landsat SLC-off products because those could bring additional artificial information in the gap-filled regions. In the annual image classification, to minimize the impact of seasonal variations, four Landsat images acquired from each season (Spring, 3–5; Summer: 6–8; Autumn: 9–11; Winter: 12–2) with lowest cloud cover for each year were selected for each mining sites. Random Forest, a supervised classification algorithm, was applied to map the land-use from moderate resolution Landsat images collected at different times. We followed the procedures described by Feng et al. (2016) for training sample collection, Random Forest classification, annual result composition and temporal consistency check. The land cover system includes cropland, other vegetation, water and hard surface. Four Landsat images from each season were classified and the four seasonal mapping results were then integrated into the annual mapping results to minimize the mapping error because of seasonal variation (data acquisition time). For example, an area is a barren land type in the dry season which may change to grassland during the wet season. In this case, the area is assigned as grassland in the annual analysis. This helps to differentiate the natural vegetation from the open pit mining area which is consistently bare throughout the year. Finally, the annual land cover mapping results were then used to identify the temporal variations in the spatial distribution of land-use classes and the land-use change for each mines.

3.3. Time-series VI/NTL analysis

Normalised Difference Vegetation Index (NDVI) is usually used for vegetation mapping. Mining-related disturbance generally cause changes in surface vegetation cover, including deforestation, and in case of reclaimed areas, afforestation, which can be detected by NDVI dynamics. A least square approach was used to fit a linear trend (i.e., increasing or decreasing) to NDVI for each mine, from the year 2000. The areas where mining activities damaged vegetation would show a negative trend, while the areas where reclamation and restoration have been carried out would show positive trends.

Because of their long time span (1992–2013), NTL dataset can also be used for long-term mining-related change detection. We selected the annual composition of NTL images from a series of satellites (i.e. F10 (1992–1994), F12 (1995–1996), F14 (1997–2003), F16 (2004–2009), and F18 (2010–2013)) due to their relatively consistent temporal trends of total digital numbers (DNs) over past two decades (Li & Zhou, 2017). The NTL time series was processed for intercalibration using the approach described in Elvidge et al. (2009) to ensure the change of yearly NTL is comparable among different years. The average digital number values for all cloud-free observations (after removing the ephemeral lights and background noise) were used in this study. The NTL detector is capable of detecting faint light sources as well as bright lights (Elvidge et al., 2014). Here, overall trends of DN values for the NTL time series at the center of a mine and in a 5-km buffer (as suggested by Kivinen, 2017), which represents the change of NTL intensity and spatial extent, respectively, were used to identify the mining-related disturbance (expand, shrink or complex) from 1992 to 2013.

4. Results and discussions

4.1. Overview

The results of the interpreted land cover change types (Expand,

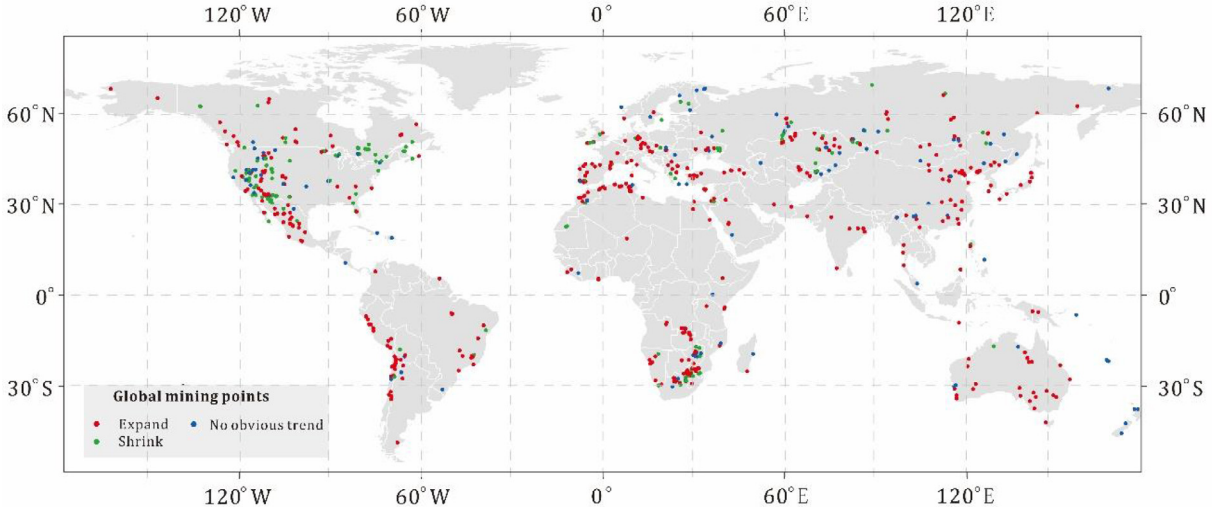

Fig. 2. Change types of surface mining spots during 2000 to 2013.

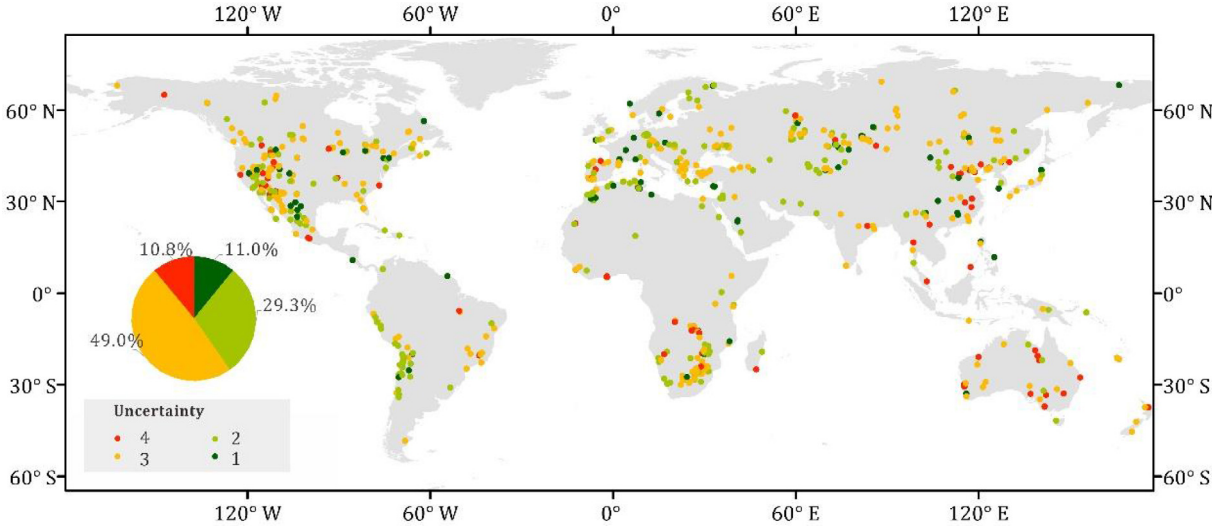

Fig. 3. Uncertainty of the change types for the mining spots.

Shrink and No obvious change) are shown for global surface mining spots in Fig. 2. We analysed the results by continents and by countries to understand region-wise trends in land cover changes. We also describe case studies and examples to demonstrate the use of multi-temporal and multi-resolution remote sensing datasets in understanding surface mining related land cover changes.

The uncertainty in the identification of the change types for mining spots is shown in Fig. 3). Here, scores 1 to 4 represents the uncertainty of mining disturbance results, from the least reliable (score of 1) to the most reliable (score of 4). Score 4 was assigned to those mining spots where all the four datasets showed a consistent change type. A score of 3 was allotted to the spots where three datasets showed consistent results. And if two of the datasets with higher resolution showed the same results while the others showed the reverse trend, or only two or three datasets detected the change, a score of 2 was assigned. The score of 1 was allotted when some of the datasets failed to detect any change or no consistent change type was found across different datasets.

Figs. 4 and 5 indicate that the count/proportion of these change

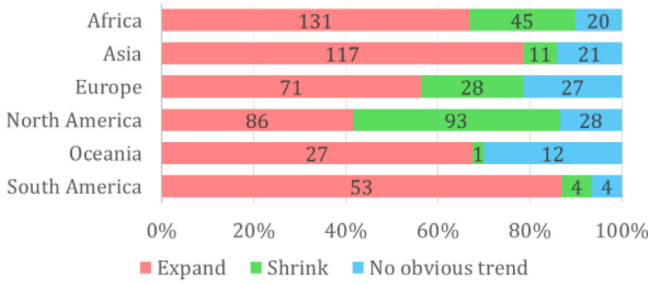

Fig. 5. Proportions of different change groups for different continents.

categories in different countries and continents respectively. North America (e.g., the United States and Canada) was the only continent to have more surface mining spots categorized as Shrink (rehabilitated) rather than Expand. South America (e.g., Chile and Brazil) and Asia

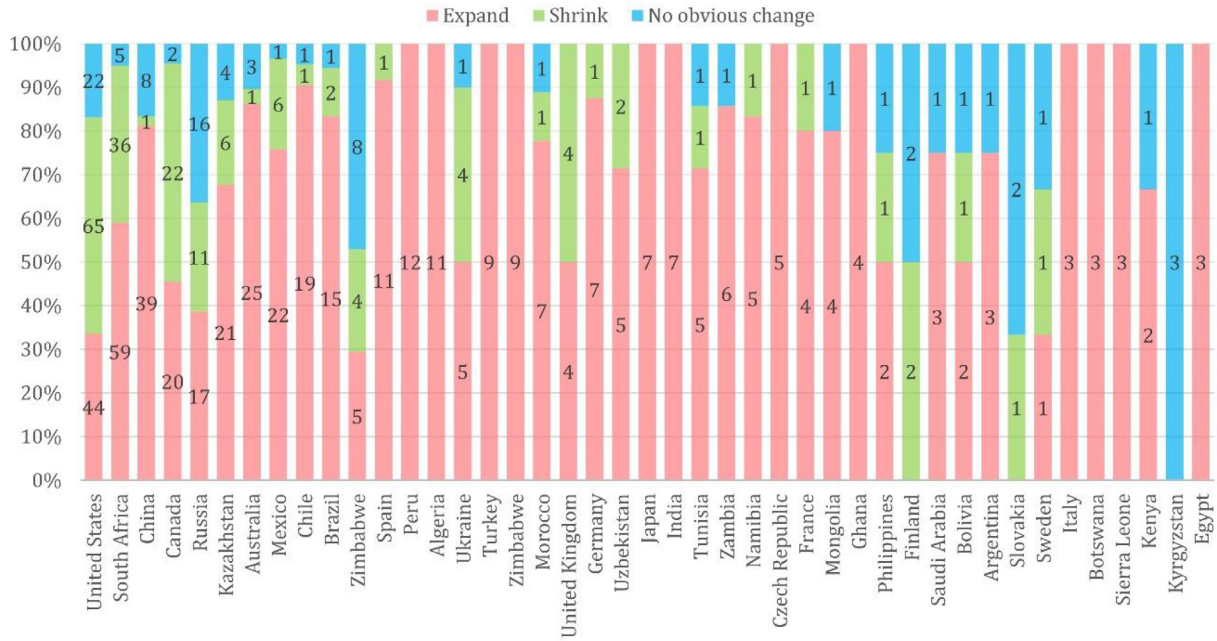

Fig. 4. Proportions of different change groups for countries with at least 3 records in the USGS MMDW database.

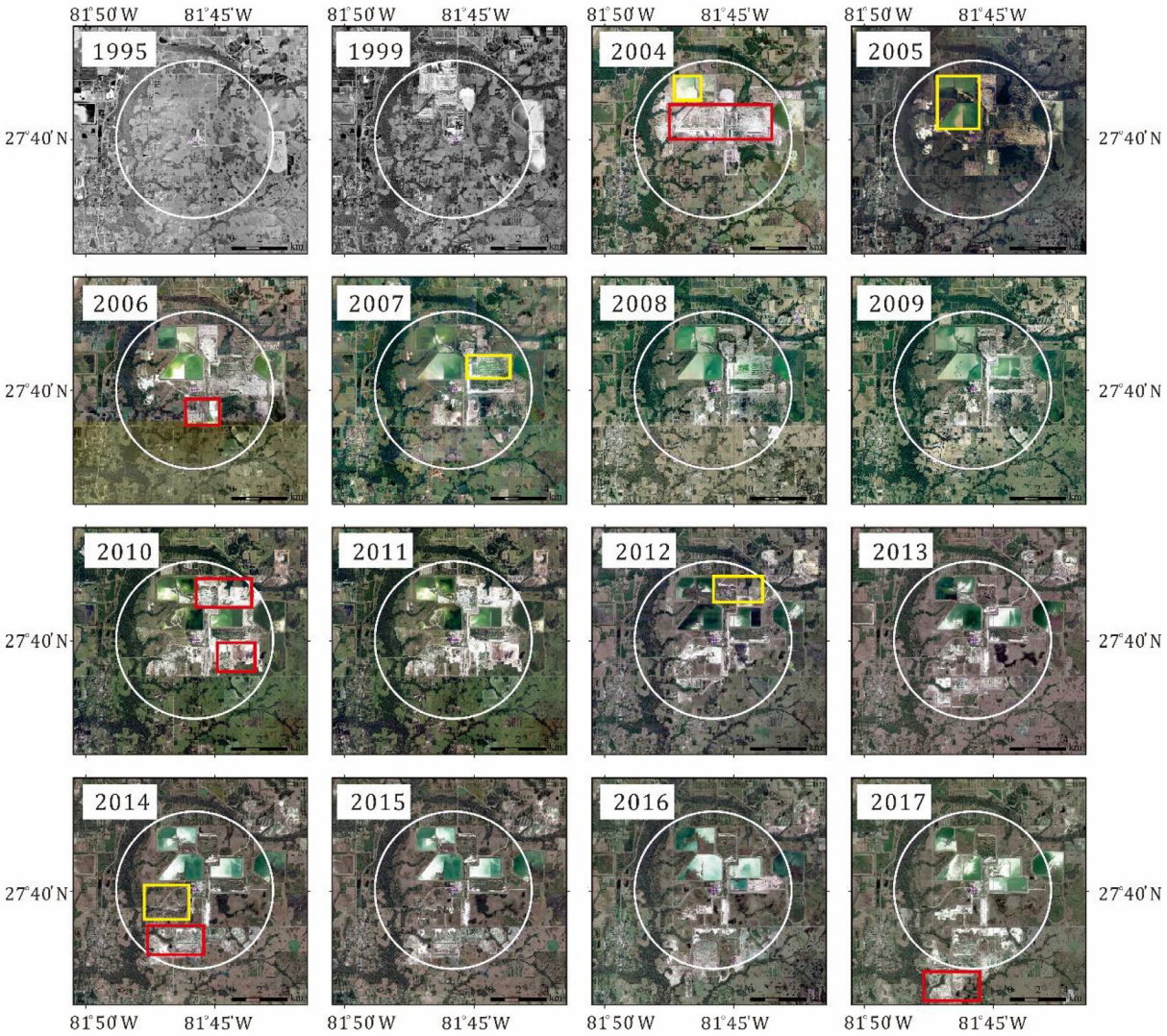

Fig. 6. Mining disturbance from high-resolution images for Fort Meade Mine – Cargill Mine, USA, from Google Earth during 1995 to 2017. Deposit ID: 701, country: United States, commodity: rock phosphate, dep_type: Marine biogenic-chemical sediment – phosphate rock.

(e.g., India and China) had the largest proportions of expanded spots. This is probably because that after long-time resource exploitation, those developed countries (i.e., the United States, Canada) began to realize the importance of environmental protection and set up the strict legislation to mine repair. For those developing countries, mining activity is an important way to maintain the living and regulation is insufficient.

Besides, the four datasets individually provided significant insights in the land-use change patterns in mining belts. Many examples with those datasets were elaborated in the following sections.

4.2. Evidence from single dataset

4.2.1. High-resolution images based example

High-resolution time series images, with finer spatial resolution, allow more detailed land use/cover information than coarse resolution product (i.e., 30-m Landsat archives and 250-m MODIS records). Here we selected Fort Meade Mine – Cargill (Id: 701), a rock phosphate mine in central Florida, USA, for our experiment. Fig. 6 shows the high-resolution images available on Google Earth from 1995 to 2017, which document the construction, expansion and rehabilitation process of the selected mining area. The white circles in the time lapse images from Google Earth mark the mining areas with rapid land cover changes. Using spectral and image characteristics such as reflectance, texture, shape, size of patches, we could identify various land-use classes such as vegetation, reservoirs and bare surface by visual interpretation. The time lapse fine resolution images from Google Earth (Fig. 6) indicate that, the rock phosphate mine was constructed in 1999. From 2004 onwards, the mine continuously expanded outwards (see the red rectangles). However, restoration of deeply excavated pits as reservoirs (see the yellow rectangles in 2004 and 2005) and of mining areas to vegetation (see the yellow rectangles in 2012 and 2014) was also detected.

4.2.2. Landsat images based example

Time series Landsat archives are widely used in monitoring land surface change such as urban sprawl (Zhang and Weng, 2016; Li et al., 2015), forest disturbance (Verbesselt et al., 2012; Schmidt et al., 2015) and cropland change (Xu et al., 2017). However, the detection of land cover changes in surface mining areas has not yet been conducted. Here an example of monitoring mining activity changes was given in Xiafangshen Mine, China, one of the largest magnesium mines in the world. After the random–forest-based classification of the Landsat TM/ETM+/OLI images, seasonal and annual land cover maps were generated for the Xiafangshen Village, Northeastern China. Fig. 7 illustrates the annual land cover mapping results for the study area (with four

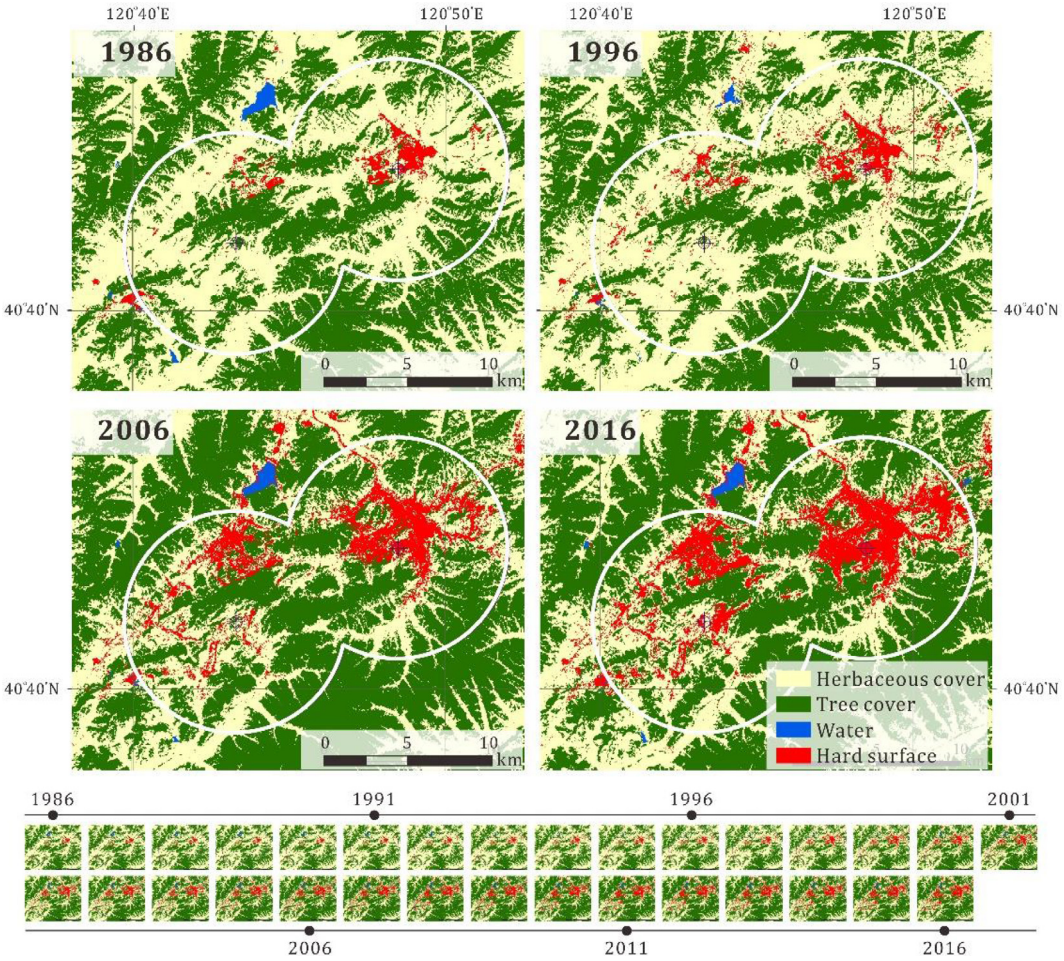

Fig. 7. Annual mapping results in Xiafangshen Mine, China using time series Landsat images from 1986 to 2016 (four selected years zoomed and others listed below). Deposit ID: 208, country: China, commodity: Magnesite, dep_type: Sedimentary.

typical years enlarged in the top frame and the whole time series results in the bottom frame) for the years 1986 to 2016. The red color in Fig. 7 represents the surface mining area, which is characterized as hard surface comprising impermeable materials as compared to the surrounding natural vegetation. The yellow, green and blue colors represent herbaceous cover, tree cover and water, respectively. The time series mapping results showed that the mining regions experienced two stages of change: 1) the area remained nearly unchanged from 1986 to 1997; and 2) the area continuously expanded from 1998 to 2016 (see the white circles in Fig. 7, the hard surface expanded at the cost of tree and herbaceous cover. The time series Landsat images not only captured the exact time point of surface mining activity expansion but also provided detailed conversion types and patterns (from natural vegetation to hard surface).

4.2.3. MODIS VI based examples

We explored the surface mining activities (expand, shrink and no obvious trend) by tracking the vegetation conditions in several surface mining spots from 2000 to 2016 using time-series MODIS VI. Fig. 8 shows the variations in vegetation index (VI) over the center of the mining spot in four typical sites over the 18 years: (a) Mulatos, gold and copper mine in Mexico; (b) Three Springs, talc and asbestos mine in Australia; (c) Fort Meade Mine – Cargill, phosphate rock mine in the United States; and (d) North Stradbroke Island, titanium-zirconium-rare earth elements (REE) mine in Australia.

Commercial production from the first site, Mulatos Mine, was launched in 2006. The long time series VIs in Fig. 8(a) effectively captures the gradual expansion of mining activities from 2006 onwards, with an apparent decline in NDVI values from ~0.25 to 0.1. The second site in Fig. 8(b) is the Three Springs deposit in Australia. Three Springs is the second largest talc mine in the world and the largest talc producer in Australia. The overall trend of VIs for the center of the mine site (deposit ID: 56) is increasing, with the lowest NDVI in 2000 and the highest in 2013. The Cargill deposit, characterized as marine chemical sediment, is located in the Central Florida District and has been exploited since the 1960s. The fluctuating VIs (higher in 2000–2004 and 2010–2012, lower in 2004–2009 and 2012–2015) in Fig. 8(c) suggest simultaneous mining as well as rehabilitation in this area. In North Stradbroke Island, mining activity has been conducted for more than 60 years. Based on Australia's National Mineral Resources Act, sand mining on the island would be phased out by 2027 and the mined land would become a national park, eventually covering 80% of the island. However, continuous decline of MODIS NDVI values indicate that mining activity was probably continued and even expanded since 2004 (Fig. 8(d)). This demonstrates that we can use the sharp decrease in VIs to detect the rapid expansion of the mining spot which may potentially damage the local environment.

4.2.4. NTL based examples

NTL based observations are potential to detect gas flaring, coal fire or other luminance caused by mining activities at night (Elvidge et al., 2009; Li, et al., 2016; Ali et al., 2017). In general, there are two sources of lights that related to the surface mining activities. Mining induced lights such as gas flaring or coal fires can be easily captured by satellites at night, particularly for those large mining sites. For instance, Elvidge et al. (2009) used the NTL time series data to explore the efficiency of

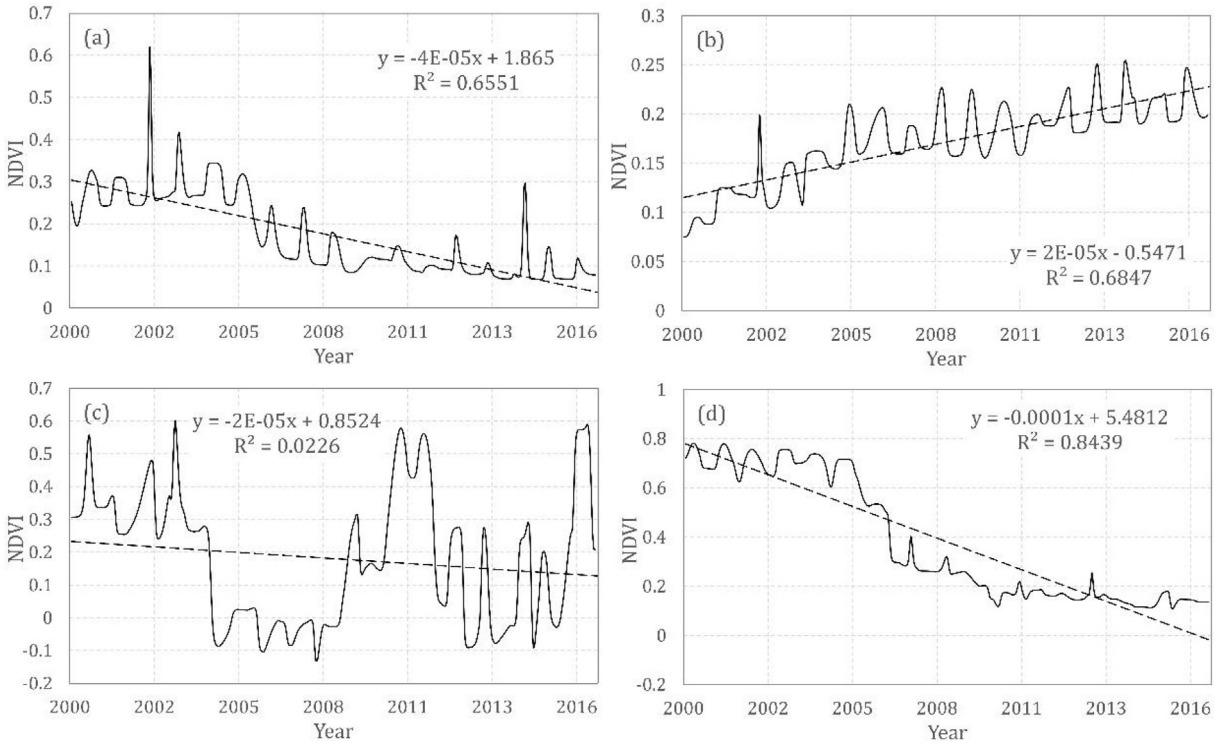

Fig. 8. Vegetation index (VI) changes in four typical surface mining spots from 2000 to 2017. (a) Deposit ID: 1213, country: Mexico, commodity: Gold, Copper, dep_type: Hydrothermal; (b) deposit ID: 56, country: Australia, commodity: Talc, Asbestos, dep_type: Unclassified; (c) deposit ID: 701, country: United States, commodity: Phosphate rock; dep_type: Sedimentary; (d) deposit ID 65, country: Australia, commodity: Titanium-zirconium-REE, dep_type: Surficial.

oil production facilities at the global scale. In addition, human settlements with electricity use at night can also be detected using NTL images. Bharti et al. (2011) used the brightness change of NTL images to analysis the dynamics of population density in west Africa. Therefore, human activities around the mining sites can also be detected using NTL time series.

NTL time series can provide an effective monitoring of active mine due to the lighting of the mine sites. Three typical cases related to NTL change are presented in Fig. 9. For a deposit in Chile (Fig. 9(a)), the overall trend of NTL (Digital Number (DN) value for the center of the mine site (deposit ID: 1103)) is increasing, with a strong signal observed around 2002. This is probably because of the intensified mining activities in this region generating brighter luminance at night. For a deposit in South Africa (Fig. 9(b)), it is clear that the DN value of the center point decreased in the period from 1992 to 2013. Given that this is a mining location, it is likely that the mining activities slowed down gradually, then significantly after 2002 as the observed DN value after 2002 was decreased rapidly. For a deposit in Finland (Fig. 9(c)), the NTL time series was relatively stable over the whole period. Therefore, it is likely that stable mining activity was ongoing throughout the whole period.

Fig. 10 demonstrates the integration of NTL and Landsat data towards the monitoring of mining activities for four different mining spots (a), (b), (c) and (d). In each of the subfigures, the top three shows NTL changes in a 5-km buffer of the observed mine site, NTL (DN values) in the first year (1992/1995) and NTL in the final year (2013), respectively, and the bottom shows the corresponding Landsat images in the same year. The NTL changes were calculated using a linear trend (i.e., increasing or decreasing) of DN values for each pixel between 1992/1995 and 2013. Red color in the first column of Fig. 10 (a), (b). (c) and (d) refers to decreasing trend of NTL and the green one is the increasing trend. This figure shows how NTL perform the mining

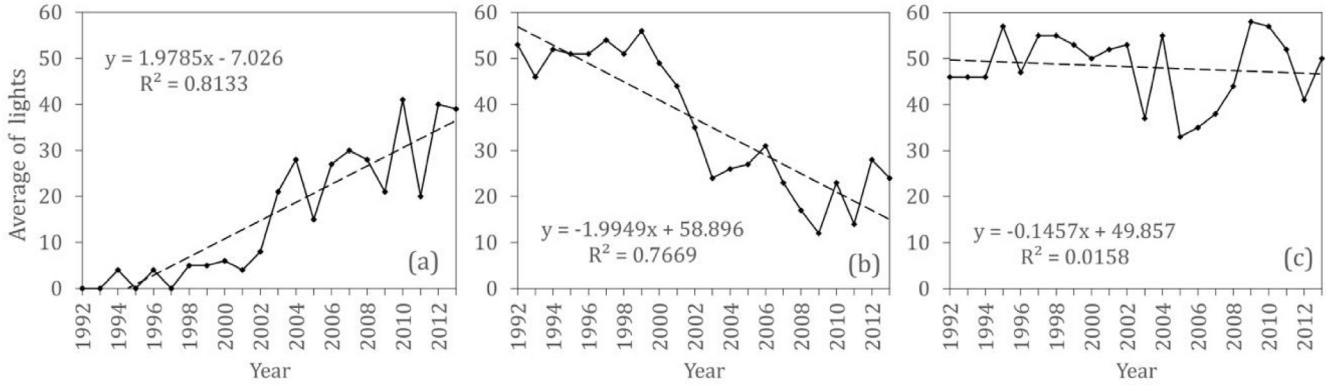

Fig. 9. Three typical cases related to NTL change with NTL time series, (a) deposit ID: 1103, country: Chile, commodity: Copper, molybdenum, dep_type: Hydrothermal; (b) deposit ID: 2785, country: South Africa, commodity: Gold, PGE, Silver, dep_type: Surfacial; (c) deposit ID: 1324, country: Finland, commodity: Tungsten, dep_type: Sedimentary.

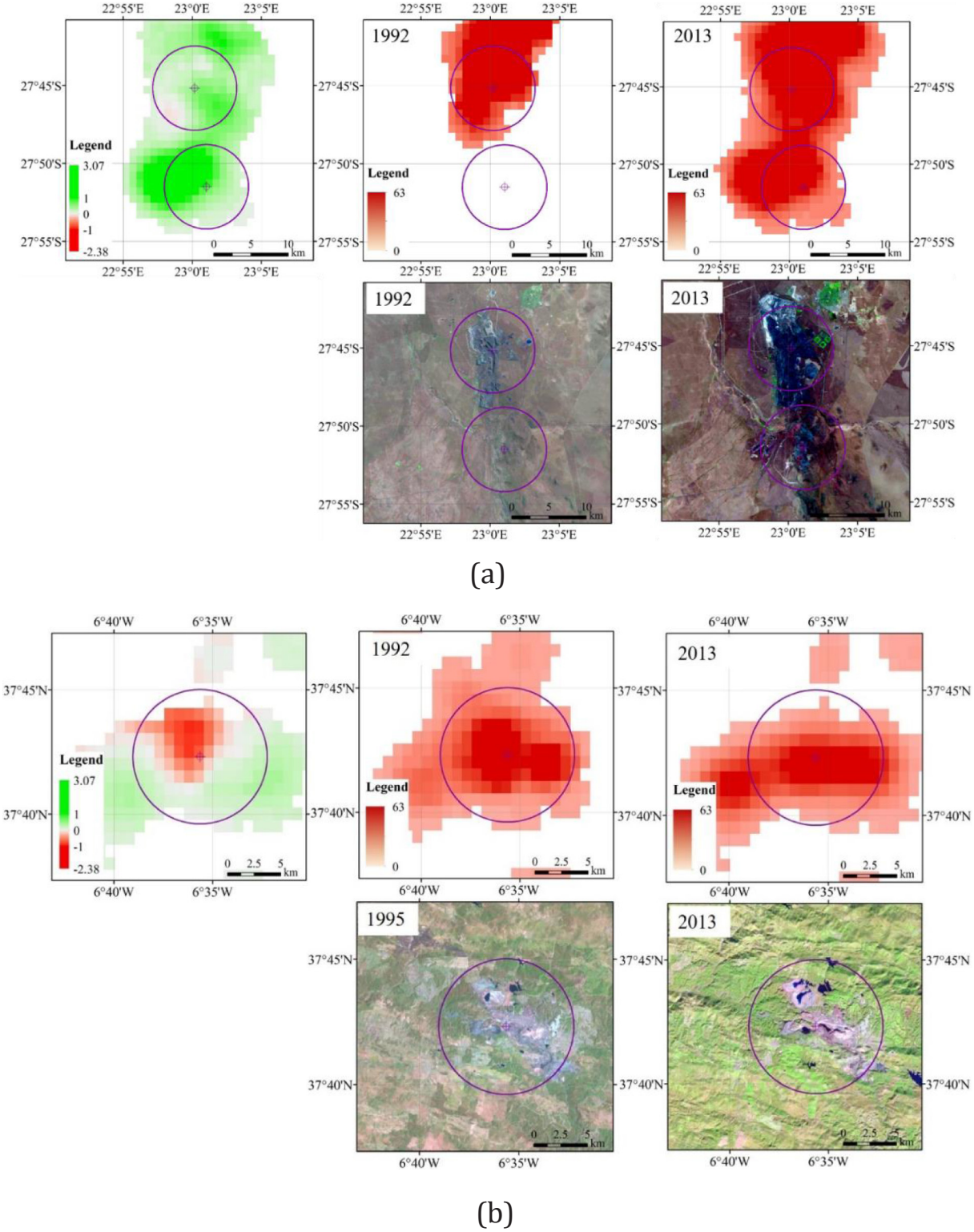

Fig. 10. Four cases related to nighttime light change, i.e. (a) deposit ID: 2837, country: South Africa, commodity: Iron, dep_type: Sedimentary, increased NTL change type: expand; (b) deposit ID: 1829, country: Spain, commodity: Copper, dep_type: Hydrothermal, decreased NTL, change type: shrink; (c) deposit ID: 40, country: Australia, commodity: Iron, dep_type: Sedimentary, stable NTL; (d) deposit ID: 1119, country: Chile, commodity: Copper, gold, dep_type: Hydrothermal, increased NTL, change type: expand.

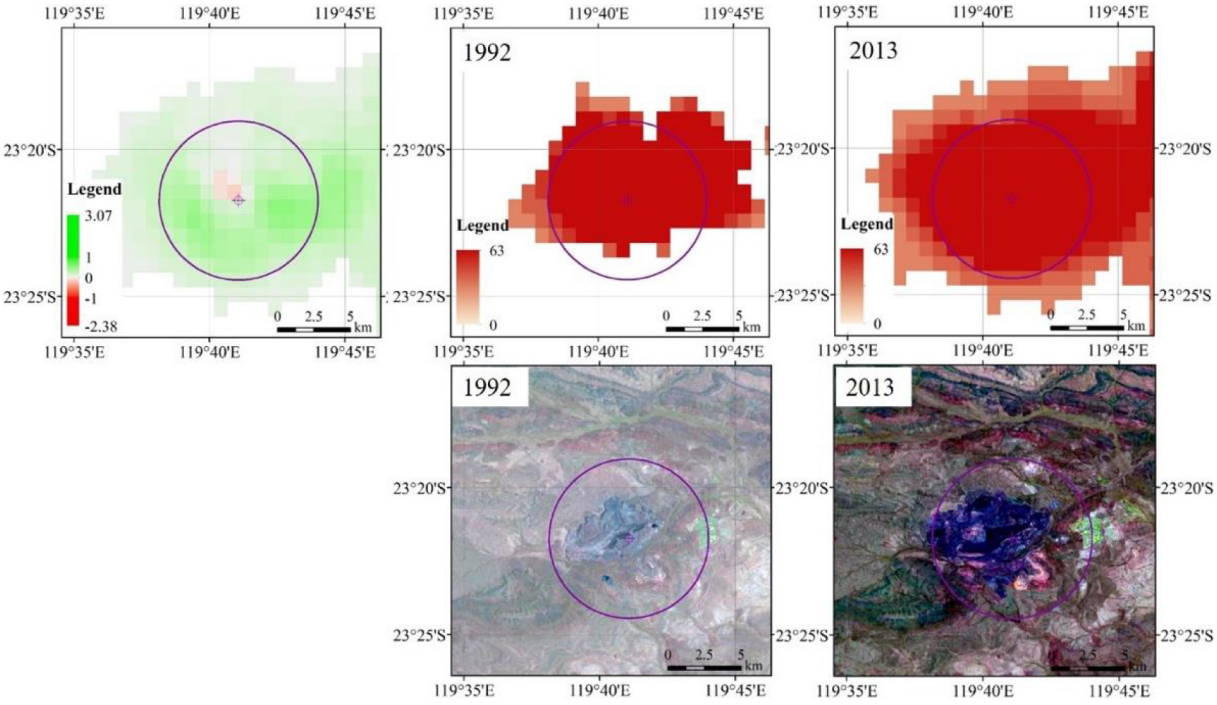

(c)

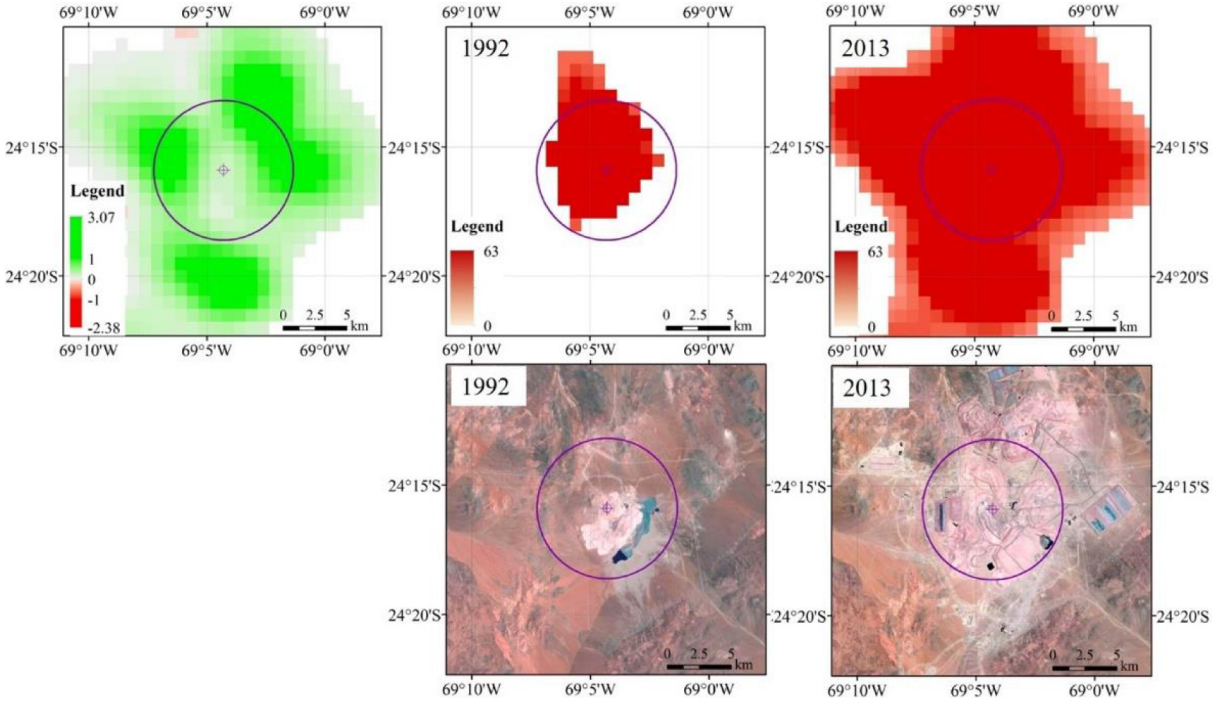

(d)

Fig. 10. (*continued*)

disturbance and the similar results by the referring Landsat images.

(a) This site is located in South Africa. Overall, there are two active mines (As the two circle shows in Fig. 10a). By combining the NTL trend and two-period Landsat images, it can be shown that the mining spot started in the north which is then shifted to the south. A more distinct increment of NTL can be found in the southern part. Also, the Landsat images indicate that the initial bare land has been

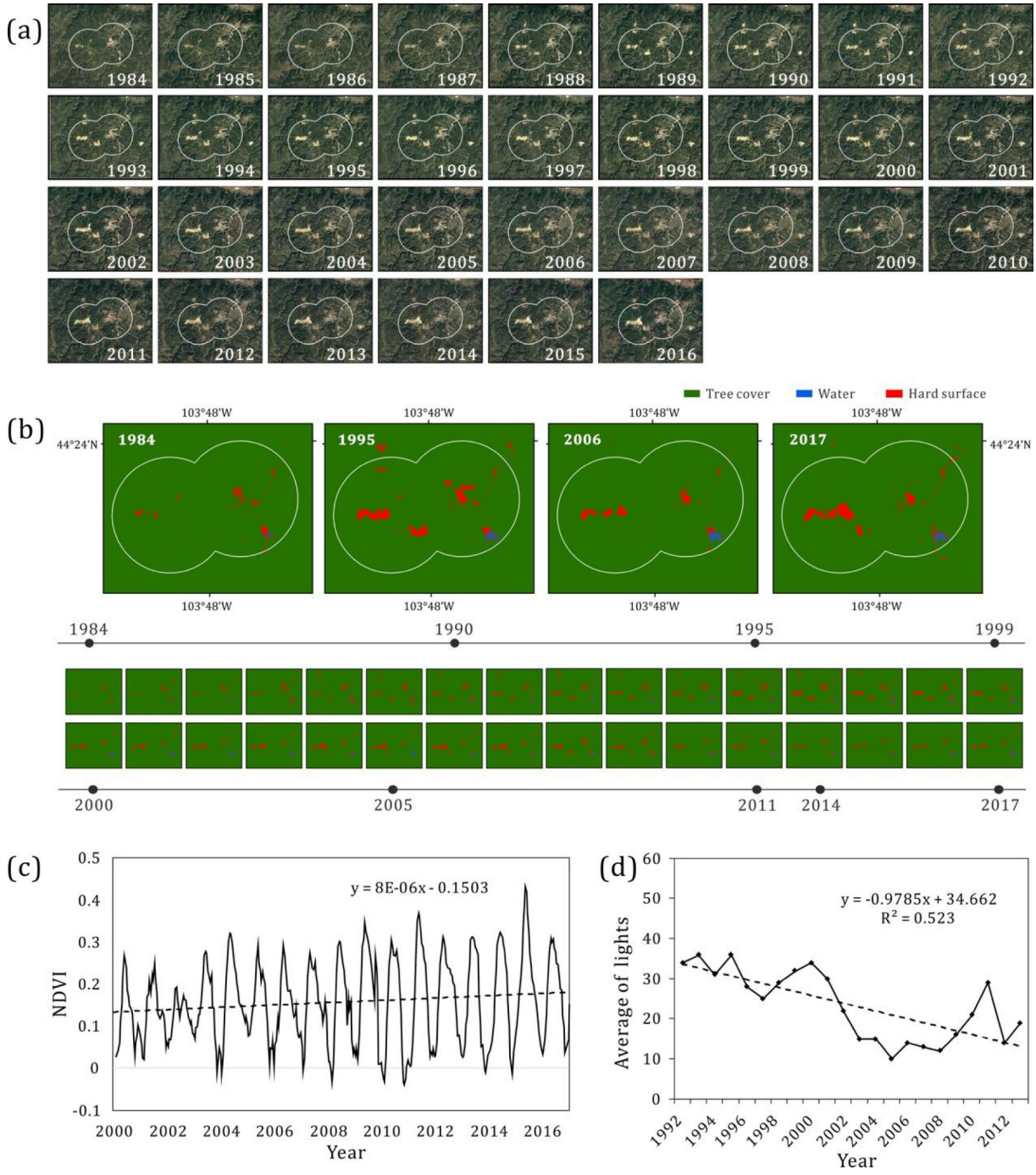

Fig. 11. Mining disturbance for Bald Mountain (Wharf, Trojan, Portland), USA from (a) high-resolution images from Google Earth (1984–2016); (b) annual mapping results using time series Landsat images (1984–2017); (c) vegetation index (VI) changes from 2000 to 2017; (d) nighttime light time series (during 1992 to 2012). Deposit ID: 2184, 2187, country: United States, commodity: gold, silver, dep_type: Gold, silver.

converted to mining spots with relatively high reflectance.

(b) This site exhibits a clear correspondence between NTL, mine locations in Landsat images. The North-West part in the circle shows a clear decreasing trend whereas for the remaining area, the mean DN slightly increased. Therefore, it is likely that the main mining region was centered around the shrinking area (red color in Fig. 10b-i), which is closer to the water (dark blue in Fig. 10b-iv and 9b-v) for practical mining activities.

(c) This is a case where the mining activities in this region were relatively stable without considerable shift in DN change over the past decades. The mean DN value in the mining region is only slightly decreasing (~0.1 in Fig. 10c-i).

(d) This is a region with expanding mining regions in Chile. The change in NTL in the central part of the circle is quite stable, whereas its surrounding region shows an increasing trend. The expanded mining region was clear when referring to the two-date Landsat images.

4.3. Comparison of results of all four datasets

In this section, we explore the mining-related land cover disturbance using high-resolution images from Google Earth, time series Landsat images/VI/NTL and compare their performance. Fig. 11 demonstrates the land type changes in a deposit located in the USA

(deposit ID: 2184 and 2187) during 1984 to 2017 using all four datasets. The three datasets (Google Earth, Landsat and Nighttime light) showed a consistent trend of increasing land cover disturbance in the past ~3 decades for the studied mine site. The recovery of vegetation is detected in four time-series datasets after 2000. Both high- and moderate-resolution datasets showed a significant expansion in 1980s, followed by a stable period in 1990s. However, there is some difference between the results obtained from the four datasets. For example, the fluctuations land recovery in mining areas in 1990s as interpreted from the time-series NTL, are different from those interpreted from high resolution images. After 2000, the recovery is more obvious in the annual mapping results derived from Landsat images and time series MODIS VI/NTL as compared to the higher resolution images from Google Earth. However, overall, all the four datasets showed a consistent tendency.

5. Conclusions

This study presented a global surface mining dataset with accurate spatial location and changes in mining footprint. Multiple remote sensing datasets (high-resolution images in Google Earth, Landsat TM/ETM +/OLI, MODIS VI, DMSP/NTL) with long-term observations were used to investigate the land changes in mining areas around the world from 1980s to 2013. However, because of the lack of availability of global high spatial resolution and high temporal resolution datasets, only a small subset of all surface mining operations was covered in the current study and the reliability of the result depends largely by the spatial/temporal resolution of the available data. Nevertheless, this study proposes and demonstrates a workflow for analyzing and integrating different types of readily available remote sensing images in order to understand the global patterns of land use changes driven by mining activities. In the future, repeated observations from higher resolution images (e.g., Planet Labs Inc., https://www.planet.com/) can be integrated into the workflow proposed in this study.

North America (e.g., the United States and Canada) was the only continent to have more surface mining spots categorized as shrink (rehabilitated) type rather than expand type in the most recent two decades. South America (e.g., Chile and Brazil) and Asia (e.g., India and China) have the highest proportions of expanded spots. Conflicts among mining and the surrounding environment/ecosystem services need to be addressed, especially for countries in South America, Asia, and Africa, where high proportions of expanded spots were detected. This study can help in prioritizing mining spots for taking corrective actions by appropriate agencies in these countries.

Acknowledgments

This research was partially supported by the National Key R&D Program of China (No. 2017YFA0604401) and the research grant from Tsinghua University (grant number: 20151080351).

References

Ali, A., Strezov, V., Davies, P., Wright, I., 2017. Environmental impact of coal mining and coal seam gas production on surface water quality in the Sydney basin, Australia. Environ. Monit. Assess. 189, 408.

Antwi, E.K., Krawczynski, R., Wiegleb, G., 2008. Detecting the effect of disturbance on habitat diversity and land cover change in a post-mining area using GIS. Landscape Urban Plann. 87, 22–32.

Bao, N., Lechner, A.M., Johansen, K., Ye, B., 2014. Object-based classification of semi-arid vegetation to support mine rehabilitation and monitoring. J. Appl. Remote Sens. 8, 083564.

Bharti, N., et al., 2011. Explaining seasonal fluctuations of measles in niger using nighttime lights imagery. Science 334 (6061), 1424–1427.

Chen, W., Li, X., He, H., Wang, L., 2018. A review of fine-scale land use and land cover classification in open-pit mining areas by remote sensing techniques. Remote Sensing 10, 15.

Cunningham, Charles G., Zientek, Michael L., Bawiec, Walter J., Orris, Greta J., 2005. Geology and Nonfuel Mineral Deposits of Latin America and Canada: Open-File Report 2005-1294-B. U.S. Geological Survey, Reston, Virginia.

Demirel, N., Emil, M.K., Duzgun, H.S., 2011. Surface coal mine area monitoring using multi-temporal high-resolution satellite imagery. Int. J. Coal Geol. 86, 3–11.

Elvidge, C., Ziskin, D., Baugh, K., Tuttle, B., Ghosh, T., Pack, D., Erwin, E., Zhizhin, M., 2009. A fifteen year record of global natural gas flaring derived from satellite data. Energies 2, 595.

Elvidge, C.D., Hsu, F.-C., Baugh, K.E., Ghosh, T., 2014. National trends in satellite-observed lighting. Global urban monitoring and assessment through earth observation 23, 97–118.

Erener, A., 2011. Remote sensing of vegetation health for reclaimed areas of Seyitömer open cast coal mine. Int. J. Coal Geol. 86, 20–26.

Gong, P., Wang, J., Yu, L., Zhao, Y., Zhao, Y., Liang, L., Niu, Z., Huang, X., Fu, H., Liu, S., Li, C., Li, X., Fu, W., Liu, C., Xu, Y., Wang, X., Cheng, Q., Hu, L., Yao, W., Zhang, H., Zhu, P., Zhao, Z., Zhang, H., Zheng, Y., Ji, L., Zhang, Y., Chen, H., Yan, A., Guo, J., Yu, L., Wang, L., Liu, X., Shi, T., Zhu, M., Chen, Y., Yang, G., Tang, P., Xu, B., Ciri, C., Clinton, N., Zhu, Z., Chen, J., Chen, J., 2013. Finer resolution observation and monitoring of global land cover: first mapping results with Landsat TM and ETM+ data. Int. J. Remote Sens. 34 (7), 2607–2654.

Kivinen, S., 2017. Sustainable post-mining land use: are closed metal mines abandoned or re-used space? Sustainability 9, 1705. https://doi.org/10.3390/su9101705.

LaJeunesse Connette, K., Connette, G., Bernd, A., Phyo, P., Aung, K., Tun, Y., Thein, Z., Horning, N., Leimgruber, P., Songer, M., 2016. Assessment of mining extent and expansion in Myanmar based on freely-available satellite imagery. Remote Sensing 8, 912.

Latifovic, R., Fytas, K., Chen, J., Paraszczak, J., 2005. Assessing land cover change resulting from large surface mining development. Int. J. Appl. Earth Obs. Geoinf. 7, 29–48.

Lechner, A.M., Kassulke, O., Unger, C., 2016. Spatial assessment of open cut coal mining progressive rehabilitation to support the monitoring of rehabilitation liabilities. Resour. Policy 50, 234–243.

Li, J., Zipper, C.E., Donovan, P.F., Wynne, R.H., Oliphant, A.J., 2015. Reconstructing disturbance history for an intensively mined region by time-series analysis of Landsat imagery. Environ. Monit. Assess. 187, 557.

Li, D., Zhao, X., Li, X., 2016. Remote sensing of human beings – a perspective from nighttime light. Geo-spatial Inform. Sci. 19 (1), 69–79.

Li, X.C., Zhou, Y.Y., 2017. A stepwise calibration of global DMSP/OLS Stable Nighttime Light Data (1992–2013). Remote Sensing 9, 637.

Malaviya, S., Munsi, M., Oinam, G., Joshi, P.K., 2010. Landscape approach for quantifying land use land cover change (1972–2006) and habitat diversity in a mining area in Central India (Bokaro, Jharkhand). Environ. Monit. Assess. 170, 215–229.

Masek, J.G., Vermote, E.F., Saleous, N.E., Wolfe, R., Hall, F.G., Huemmrich, K.F., Gao, J., Lim, T.K., 2006. A Landsat surface reflectance dataset for North America, 1990–2000. IEEE Geosci. Remote Sens. Lett. 3 (1), 68–72.

Nokleberg, Warren J., Bawiec, Walter J., Doebrich, Jeff L., Lipin, Bruce R., Miller, Robert J., Orris, Greta J., Zientek, Michael L., 2005. Geology and nonfuel mineral deposits of Greenland, Europe, Russia, and northern Central Asia: Open-File Report 2005-1294-D. U.S. Geological Survey, Reston, Virginia.

Pei, W., Yao, S., Knight, J.F., Dong, S., Pelletier, K., Rampi, L.P., Wang, Y., Klassen, J., 2017. Mapping and detection of land use change in a coal mining area using object-based image analysis. Environ. Earth Sci. 76, 125.

Petropoulos, G.P., Partsinevelos, P., Mitraka, Z., 2013. Change detection of surface mining activity and reclamation based on a machine learning approach of multi-temporal Landsat TM imagery. Geocarto International 28, 323–342.

Peters, Stephen G., Nokleberg, Warren J., Doebrich, Jeff L., Bawiec, Walter J., Orris, Greta, Sutphin, David M., Wilburn, David R., 2005. Geology and Nonfuel Mineral Deposits of Asia and the Pacific: Open-File Report 2005-1294-C. U.S. Geological Survey, Reston, Virginia.

Raval, S., Shamsoddini, A., 2014. A monitoring framework for land use around kaolin mining areas through Landsat TM images. Earth Sci. Inf. 7, 153–163.

Redondo-Vega, J.M., Gómez-Villar, A., Santos-González, J., González-Gutiérrez, R.B., Álvarez-Martínez, J., 2017. Changes in land use due to mining in the north-western mountains of Spain during the previous 50years. CATENA 149, 844–856.

Schmid, T., Rico, C., Rodríguez-Rastrero, M., José Sierra, M., Javier Díaz-Puente, F., Pelayo, M., Millán, R., 2013. Monitoring of the mercury mining site Almadén implementing remote sensing technologies. Environ. Res. 125, 92–102.

Schueler, V., Kuemmerle, T., Shroder, H., 2011. Impacts of surface mining on land use systems in Western Ghana. Ambio 40, 528–539.

Schulz, K.J., Briskey, J.A., 2005. Major Mineral Deposits of the World: Open-File Report 2005-1294. U.S. Geological Survey, Reston, Virginia.

Soulard, C.E., Acevedo, W., Stehman, S.V., Parker, O.P., 2016. Mapping extent and change in surface mines within the United States for 2001 to 2006. Land Degrad. Dev. 27, 248–257.

Taylor, Cliff D., Schulz, Klaus J., Doebrich, Jeff L., Orris, Greta, Denning, Paul D., Kirschbaum, Michael J., 2009. Geology and Nonfuel Mineral Deposits of Africa and the Middle East: Open-File Report 2005-1294. U.S. Geological Survey, Reston, Virginia.

Townsend, P.A., Helmers, D.P., Kingdon, C.C., McNeil, B.E., de Beurs, K.M.M., Eshleman, K.N., 2009. Changes in the extent of surface mining and reclamation in the Central Appalachians detected using a 1976-2006 Landsat time series. Remote Sensing Envrion. 113, 62–72.

Verbesselt, J., Zeileis, A., Herold, M., 2012. Near real-time disturbance detection using satellite image time series. Remote Sens. Environ. 123, 98–108.

Xu, Y., Yu, L., Zhao, Y., Feng, D., Cheng, Y., Cai, X., Gong, P., 2017. Monitoring cropland changes along the Nile River in Egypt over past three decades (1984–2015) using remote sensing. Int. J. Remote Sens. 38 (15), 4459–4480.

Yang, Y., Erskine, P.D., Lechner, A.M., Mulligan, D., Zhang, S., Wang, Z., 2018. Detecting

the dynamics of vegetation disturbance and recovery in surface mining area via Landsat imagery and LandTrendr algorithm. J. Cleaner Prod. 178, 353–362.
Yu, L., Gong, P., 2012. Google Earth as a virtual globe tool for earth science applications at global scale: progress and perspectives. Int. J. Remote Sens. 33 (12), 3966–3986.
Yu, L., Liang, L., Wang, J., Zhao, Y., Cheng, Q., Hu, L., Liu, S., Yu, L., Wang, X., Zhu, P., Li, X., Xu, Y., Li, C., Fu, W., Li, X., Li, W., Liu, C., Cong, N., Zhang, H., Sun, F., Bi, X., Xin, Q., Li, D., Yan, D., Zhu, Z., Goodchild, M.F., Gong, P., 2014a. Meta-discoveries from a synthesis of satellite-based land cover mapping research. Int. J. Remote Sens. 35 (13), 4573–4588.
Yu, L., Wang, J., Gong, P., 2013. Improving 30 meter global land cover map FROM-GLC with time series MODIS and auxiliary datasets: a segmentation based approach. Int. J. Remote Sens. 34 (16), 5851–5867.
Yu, L., Wang, J., Li, X., Li, C., Gong, P., 2014b. A multi-resolution global land cover dataset through multisource data aggregation. Science China Earth Sci. 57 (10), 2317–2329.
Zhang, L., Weng, Q., 2016. Annual dynamics of impervious surface in the Pearl River Delta, China, from 1988 to 2013, using time series Landsat imagery. ISPRS J. Photogramm. Remote Sens. 113, 86–96.
Zientek, Michael L., Orris, Greta J., 2005. Geology and nonfuel mineral deposits of the United States: Open-File Report 2005-1294-A. U.S. Geological Survey, Reston, Virginia.